

Eight-stage pseudo-symplectic Runge–Kutta methods of order (4, 8)

Misha Stepanov

stepanov@arizona.edu

*Department of Mathematics and Program in Applied Mathematics,
University of Arizona, Tucson, AZ 85721, USA*

Abstract

Using simplifying assumptions that are related to the time reversal symmetry, a 1-dimensional family of 8-stage pseudo-symplectic Runge–Kutta methods of order (4, 8), *i.e.*, methods of order 4 that preserve symplectic structure up to order 8, is derived. An example of 7-stage method of order (4, 9) is given.

Keywords: pseudo-symplectic Runge–Kutta methods

MSC Classification: 65L05 , 65L06

Runge–Kutta methods (see, *e.g.*, (Butcher, 2016, s. 23 and ch. 3), (Hairer *et al.*, 1993, ch. II), (Ascher & Petzold, 1998, ch. 4), (Iserles, 2008, ch. 3)) are widely and successfully used to solve ordinary differential equations numerically for over a century (Butcher & Wanner, 1996). Being applied to a system $\mathbf{dx}/dt = \mathbf{f}(t, \mathbf{x})$, in order to propagate by the step size h and update the position, $\mathbf{x}(t) \mapsto \tilde{\mathbf{x}}(t+h)$, where $\tilde{\mathbf{x}}(t+h)$ is a numerical approximation to the exact solution $\mathbf{x}(t+h)$, an s -stage Runge–Kutta method (which is determined by the coefficients a_{ij} , weights b_j , and nodes c_i) would form the following system of equations for $\mathbf{X}_1, \mathbf{X}_2, \dots, \mathbf{X}_s$:

$$\mathbf{X}_i = \mathbf{x}(t) + h \sum_{j=1}^s a_{ij} \mathbf{F}_j, \quad \mathbf{F}_i = \mathbf{f}(t + c_i h, \mathbf{X}_i), \quad i = 1, 2, \dots, s$$

solve it, and then compute $\tilde{\mathbf{x}}(t+h) = \mathbf{x}(t) + h \sum_{j=1}^s b_j \mathbf{F}_j$. In the limit $h \rightarrow 0$ all the vectors \mathbf{F}_i , where $1 \leq i \leq s$, are the same, so it is natural and will be assumed that $\sum_{j=1}^s a_{ij} = c_i$ for all i .

It is a common wisdom that whenever a numerically simulated system has a conservation law, in order to get sensible results it is often desirable to use so-called conservative schemes, *i.e.*, the ones that preserve the conserved quantity exactly (up to round-off errors). A practically important case is when the system is Hamiltonian (Arnold, 1989, ch. 8), (Hairer *et al.*, 2006, s. VI.1), (Butcher, 2021, p. 251). Integration methods are called symplectic if they conserve the symplectic structure.

Let $\mathbf{M} = [m_{ij}]$ be the $s \times s$ matrix with $m_{ij} = b_i a_{ij} + b_j a_{ji} - b_i b_j$ as its matrix element in the i^{th} row and j^{th} column (see, *e.g.*, (Butcher, 1975), (Burrage & Butcher,

1979, eq. (2.2)), (Cooper, 1987), (Butcher, 2016, s. 390), (Hairer *et al.*, 1993, p. 316), (Iserles, 2008, p. 79), (Butcher, 2021, p. 253)). A Runge–Kutta method is symplectic if \mathbf{M} is a zero matrix \mathbf{O} , and only if it is equivalent to a method with $\mathbf{M} = \mathbf{O}$, as was independently shown by several authors: (Sanz-Serna, 1988), (Suris, 1988), (Suris, 1989), (Lasagni, 1988).¹

Unless a Hamiltonian is of a special type, *e.g.*, as it often happens in problems coming from classical mechanics, is separable: $\mathcal{H}(\mathbf{p}, \mathbf{x}) = T(\mathbf{p}) + U(\mathbf{x})$, where \mathbf{x} and \mathbf{p} are canonical coordinates, symplectic methods are implicit. In (Aubry & Chartier, 1998a) the concept of so-called pseudo-symplectic methods was introduced. A method is said to be of pseudo-symplectic order (p, q) if it is of order p (for order conditions see, *e.g.*, (Butcher, 2016, p. 172), (Butcher, 2021, p. 126), (Hairer *et al.*, 1993, p. 148)), and the symplectic structure is conserved up to the order q (see, *e.g.*, (Aubry & Chartier, 1998a, eqs. (2.5), (2.7), and tab. 2.1)).² It was shown that methods with $q \geq 2p$ have better Hamiltonian conservation properties (Aubry & Chartier, 1998a, thm. 2.6), and an explicit 5-stage pseudo-symplectic Runge–Kutta method of order $(3, 6)$ was constructed (Aubry & Chartier, 1998a, fig. 4.1).

With an abundance of implicit symplectic Runge–Kutta methods, it is only explicit pseudo-symplectic methods that are of practical interest. There is no 6-stage method of order $(4, 8)$ (Aubry & Chartier, 1998a, prop. 4.2) (see also (Aubry & Chartier, 1998b, thm. 3.3)), but there are known 6-stage methods of order $(4, 7)$: (Calvo *et al.*, 2010, p. 262) and (Capuano *et al.*, 2017, p. 90).

The aim of this work is to construct a pseudo-symplectic method of order $(4, 8)$. Order conditions are discussed in Section 1. A 1-dimensional family of 8-stage pseudo-symplectic methods of order $(4, 8)$ is derived in Section 2. The efficiency of new methods is tested on three numerical examples in Section 3.

1 Order conditions

The element-wise product of column vectors \mathbf{x} and \mathbf{y} will be denoted as $\mathbf{x} \cdot \mathbf{y}$, *i.e.*, $(\mathbf{x} \cdot \mathbf{y})_i = x_i y_i$. The element-wise product of n copies of vector \mathbf{x} will be written as \mathbf{x}^n . Let $\mathbf{1}$ be the s -dimensional column vector with all components being equal to 1; $\mathbf{A} = [a_{ij}]$ be the $s \times s$ matrix with a_{ij} as its matrix element in the i^{th} row and j^{th} column; $\mathbf{b} = [b_j]$ be the weights row vector; and $\mathbf{c} = [c_i]$ be the nodes vector. Let $\mathbf{q}_n = \mathbf{A} \mathbf{c}^n - \frac{1}{n+1} \mathbf{c}^{n+1}$, *e.g.*, $\mathbf{q}_0 = \mathbf{0}$ as $\mathbf{A} \mathbf{1} = \mathbf{c}$.

Given rooted trees t_1, t_2, \dots, t_n , a new tree $[t_1 t_2 \dots t_n]$ is obtained by connecting with n edges their roots to a new vertex, the latter becomes a new root (Butcher, 2016, s. 301), (Hairer *et al.*, 1993, p. 152), (Butcher, 2021, p. 44), (Hairer *et al.*, 2006, p. 53). Consider a vector function $\Phi : T \rightarrow \mathbf{R}^s$ on the set of rooted trees that is recursively defined as $\Phi(\bullet) = \mathbf{1}$ and $\Phi([t_1 t_2 \dots t_n]) = \prod_{m=1}^n \mathbf{A} \Phi(t_m)$, where the product of vectors is taken element-wise. This function coincides with *derivative weights* (Butcher, 2016, def. 312A), (Hairer *et al.*, 1993, pp. 148 and 151), (Aubry






¹ An S -reducible (see, *e.g.*, (Hairer & Wanner, 1996, p. 188)) 2-stage method with $a_{11} = a_{22} = b_1 = b_2 = c_1 = c_2 = \frac{1}{2}$ and $a_{12} = a_{21} = 0$ has $m_{11} = m_{22} = -m_{12} = -m_{21} = \frac{1}{3} \neq 0$. It is equivalent to the midpoint method and is symplectic.

² In (Aubry & Chartier, 1998a, eq. (2.7)) “ $(t, t') \in \hat{T}(k) \times \hat{T}(k)$ ” should be read as “ $(t, t') \in \hat{T}(k)$ ”.

& Chartier, 1998a, def. 2.2), it is closely related to *internal* or *stage weights* $\mathbf{A}\Phi(t)$ (Butcher, 2021, p. 125) and *elementary weights* $\mathbf{b}\Phi(t)$ (Hairer *et al.*, 2006, p. 55).

Representation of analytical expressions by pictures or diagrams is often convenient and illustrative, and is used in many different contexts: countless diagram techniques in theoretical physics; group theory (see, e.g., (Cvitanović, 2008)); graphical representation of Fredholm series (Mathews & Walker, 1970, s. 11.3); and connection of derivatives with rooted trees (Cayley, 1857), which was heavily developed in the context of Runge–Kutta methods (Merson, 1957), (Butcher, 1972), (Butcher, 2016, ch. 3), (Hairer *et al.*, 1993, s. II.2), (Butcher, 2021, ch. 2), (Hairer *et al.*, 2006, ch. III), with occasional usage of picturesque trees in diagrams (Butcher, 2016, pp. 188 and 189), (Hairer *et al.*, 1993, pp. 175 and 328).

Similarly to Penrose graphical notation (Penrose, 1971), an object that is a tensor of type (m, n) will be depicted by a symbol of the object connected by lines to m and n black dots below and above it, respectively:^{3,4}

	vector $\mathbf{1}$
	$\Phi(t)$ or an arbitrary vector
	matrix \mathbf{A} and identity matrix \mathbf{I}
	weights row vector \mathbf{b}
	element-wise product of vectors

Lines coming both from below and from above to a dot produce a tensor contraction, *i.e.*, the summation over the values of the corresponding tensor index. Outer products are obtained by simply drawing objects next to each other (Penrose, 1971, p. 224).

In bra-ket notation (Dirac, 1939) vectors, linear forms, scalar and outer products (the latter is an example of an operator) are denoted through $|u\rangle$, $\langle f|$, $\langle f|u\rangle$, and $|u\rangle\langle f|$, respectively, with clear distinction between vectors and forms. In quantum mechanics the evolution is *linear*, so there is no need for branching. Similarly, the stability function $R(z) = 1 + z\mathbf{b}(\mathbf{I} - z\mathbf{A})^{-1}\mathbf{1} = 1 + z\mathbf{b}\mathbf{1} + z^2\mathbf{b}\mathbf{A}\mathbf{1} + z^3\mathbf{b}\mathbf{A}^2\mathbf{1} + \dots = 1 + \sum_{n=0}^{\infty} z^{n+1}\mathbf{b}\mathbf{A}^n\mathbf{1}$ (see, e.g., (Butcher, 2016, s. 238), (Butcher, 2021, s. 5.3), (Ascher & Petzold, 1998, s. 4.4)), which describes the behavior of a Runge–Kutta method applied to a *linear* equation $dx/dt = \lambda x$ with $z = \lambda h$ (*i.e.*, $\partial^2 f_i / \partial x_j \partial x_k = 0$), contains only the terms that correspond to rooting trees with no branching.

³ Such an up/down orientation is the reverse of the one in (Penrose, 1971), and is used here so that a tree has its root at the bottom. Not drawing the dots allows an elegant representation of Kronecker delta δ_b^a and metric tensors g^{ab} and g_{ab} (Penrose, 1971, pp. 226 and 231), while here the dots correspond to the vertices of rooted trees.

⁴ The drawings of a leaf, a root, of trees *Betula pendula* and *Larix sibirica* are by Olga Stepanova, used with permission.

For the system $\mathbf{dx}/dt = \mathbf{f}(t, \mathbf{x})$ its integral form

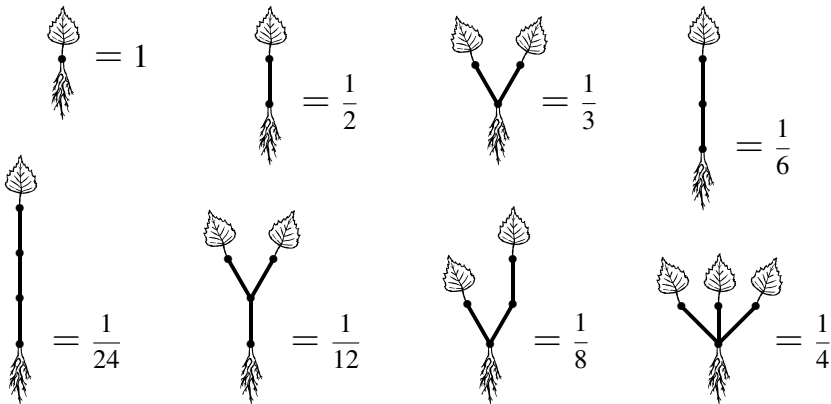
$$\mathbf{x}(t+h) = \mathbf{x}(t) + \int_t^{t+h} dt' \mathbf{f}(t', \mathbf{x}(t')) = \mathbf{x}(t) + h \int_0^1 d\theta \mathbf{f}(t + \theta h, \mathbf{x}(t + \theta h))$$

can be interpreted as the application of an idealized Runge–Kutta method with stages being indexed by an interval $[0, 1]$ (Plato’s form of a Runge–Kutta method, it is called “the Picard method” in (Butcher, 1972, p. 97), (Butcher, 2021, pp. 153 and 174)). In the upper half of the following table:

1	function $1(\theta) \equiv 1$
A	operator $u(\theta) \mapsto \int_0^\theta d\theta' u(\theta')$
b	functional $u(\theta) \mapsto \int_0^1 d\theta u(\theta)$
u.v	point-wise product $u(\theta)v(\theta)$
c	θ
q_n	0
Φ(t)	$ t \theta^{ t -1}/t!$
bΦ(t)	$1/t!$

the process/result of the substitution of entries in the left column with what is on the right will be called a *transfiguration*. It can be viewed in two ways: 1) considering quantities or statements in the idealized method; and 2) checking for desired properties of a Runge–Kutta method, such as simplifying assumptions, see, e.g., (Butcher, 1964a, p. 52), (Butcher, 2016, s. 321), (Hairer *et al.*, 1993, pp. 175, 182, and 208). Here $|t|$ is the order of tree t , i.e., the number of vertices in t . The factorial $t!$ is recursively defined as $\bullet! = 1$ and if $t = [t_1 t_2 \dots t_n]$, then $t! = |t| \prod_{m=1}^n (t_m)!$.

A Runge–Kutta method of order 4 should satisfy the order conditions $\mathbf{b}\Phi(t) = 1/t!$ for all rooted trees t with $|t| \leq 4$:



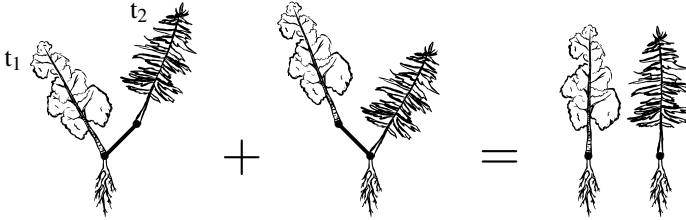
or $\mathbf{b1} = 1$, $\mathbf{bc} = \frac{1}{2}$, $\mathbf{bc}^2 = \frac{1}{3}$, $\mathbf{bAc} = \frac{1}{6}$, $\mathbf{bc}^3 = \frac{1}{4}$, $\mathbf{b(c.(Ac))} = \frac{1}{8}$, $\mathbf{bAc}^2 = \frac{1}{12}$, $\mathbf{bA}^2\mathbf{c} = \frac{1}{24}$. Consider the diagram \mathbf{bAc} in the top right statement $\mathbf{bAc} = \frac{1}{6}$. If the root or the leaf (which are there out of “all parts of the analytical expression a diagram corresponds

to are explicitly drawn” sentiment) are removed, then the diagram becomes the vector $\mathbf{Ac} = \mathbf{A}^2 \mathbf{1}$ or the row vector \mathbf{bA}^2 , respectively. If both the root and the leaf are removed, then the diagram becomes the matrix \mathbf{A}^2 . The transfiguration of, e.g., the statement $\mathbf{bAc}^2 = \frac{1}{12}$ is

$$\int_0^1 d\theta \int_0^\theta d\theta' \left(\int_0^{\theta'} d\theta'' \right) \left(\int_0^{\theta'} d\theta''' \right) = \int_0^1 d\theta \int_0^\theta d\theta' \theta'^2 = \int_0^1 d\theta \frac{\theta^3}{3} = \frac{1}{12}$$

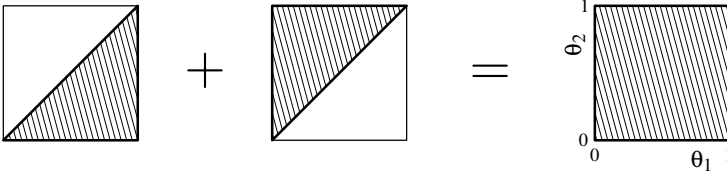
$$\mathbf{b} \quad \mathbf{A} \quad (\mathbf{A1}) \quad . \quad (\mathbf{A1}) = \mathbf{b} \quad \mathbf{A} \quad \mathbf{c}^2$$

Let $D(\Phi(t_1), \Phi(t_2))$ denote the following property (see (Aubry & Chartier, 1998a, eq. (2.5))):



$$\mathbf{b}(\Phi(t_1).(\mathbf{A}\Phi(t_2))) + \mathbf{b}((\mathbf{A}\Phi(t_1)).\Phi(t_2)) = (\mathbf{b}\Phi(t_1))(\mathbf{b}\Phi(t_2))$$

whose transfiguration or continuous analog $D(u, v)$ would be

$$\int_0^1 d\theta u(\theta) \int_0^\theta d\theta' v(\theta') + \int_0^1 d\theta \left(\int_0^\theta d\theta' u(\theta') \right) v(\theta) = \left(\int_0^1 d\theta u(\theta) \right) \left(\int_0^1 d\theta v(\theta) \right)$$


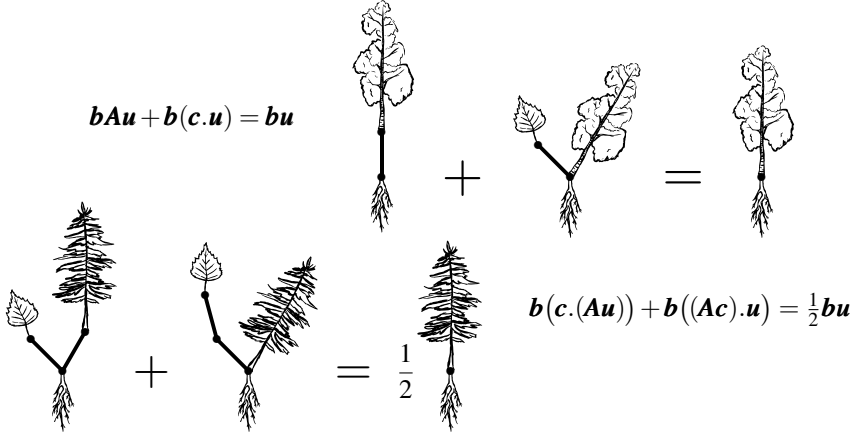
where, assuming it is $u(\theta_1)v(\theta_2)$ being integrated, the shading shows the regions of integration in the (θ_1, θ_2) -plane. Another way to interpret $D(u, v)$ is as the integration by parts formula. Consider the following bilinear form M :



whose matrix $\mathbf{M} = [m_{ij}]$, with $m_{ij} = b_i a_{ij} + b_j a_{ji} - b_i b_j$, is symmetric. The property $D(\mathbf{u}, \mathbf{v})$ can be written as $\mathbf{M}(\mathbf{u}, \mathbf{v}) = \mathbf{u}^T \mathbf{M} \mathbf{v} = 0$.

An order p Runge–Kutta method is said to be pseudo-symplectic of order (p, q) if $D(\Phi(t_1), \Phi(t_2))$ for all trees t_1 and t_2 such that $|t_1| + |t_2| \leq q$ (Aubry & Chartier, 1998a, cor. 2.2 and eq. (2.7)). B -series coefficients, $t \mapsto \mathbf{b}\Phi(t)$, for a method of order (p, q) are in the coset $(E + O_{p+1})$ and in the subgroup $(\cap_{r=1}^{q-1} D_{r, q-r})$ of the Butcher group B (Butcher, 2021, pp. 166 and 173).

The property $(D(\Phi, \mathbf{u}) \text{ for all } \mathbf{u} \in \mathbf{R}^s)$ will be shortened as $\mathbf{D}(\Phi)$ (see (Aubry & Chartier, 1998a, def. 3.1)). It is equivalent to the linear form $\mathbf{u} \mapsto M(\Phi, \mathbf{u})$ being a zero function, or $\mathbf{M}\Phi = \mathbf{0}$. The j^{th} component of $\mathbf{D}(\Phi)$, the property $D(\Phi, \mathbf{e}_j)$, where \mathbf{e}_j is the j^{th} vector of the standard basis of \mathbf{R}^s , will be denoted by $D_j(\Phi)$. Assuming that $b\mathbf{1} = 1$ and $b\mathbf{c} = \frac{1}{2}$, here are the diagrams for $\mathbf{D}(\mathbf{1})$ and $\mathbf{D}(\mathbf{c})$:



The property $\mathbf{D}(\mathbf{1})$ coincides with $D(1)$ (Butcher, 1964a, p. 52), (Butcher, 2016, fig. 321(ii)), (Hairer *et al.*, 1993, pp. 175 and 208), (Butcher, 2021, p. 193). If $C(2)$ and $D(1)$ are satisfied, then $\mathbf{D}(\mathbf{c})$ is equivalent to $D(2)$. For an explicit Runge–Kutta method that satisfies the explicit version $((\mathbf{A}\mathbf{c})_i \neq c_i^2/2) \Rightarrow ((i = 2) \wedge (b_2 = 0))$ of the property $C(2)$, it is impossible to have both $\mathbf{D}(\mathbf{1})$ and $\mathbf{D}(\mathbf{c})$ (Aubry & Chartier, 1998a, prop. 3.6).

Let a function $u(\theta)$ be called $[0, 1]$ -even or $[0, 1]$ -odd, if $u(1 - \theta) = u(\theta)$ or $u(1 - \theta) = -u(\theta)$, respectively. The following parity properties are true:

- if $u(\theta)$ is $[0, 1]$ -odd, then $U(\theta) = \int_0^\theta d\theta' u(\theta')$ is $[0, 1]$ -even
- if $u(\theta)$ is $[0, 1]$ -even and $\int_0^1 d\theta u(\theta) = 0$, then $U(\theta) = \int_0^\theta d\theta' u(\theta')$ is $[0, 1]$ -odd (1)

2 Family of pseudo-symplectic methods

A pseudo-symplectic Runge–Kutta method of order (4, 8) will be searched for within 8-stage explicit methods with $c_4 = c_5 = \frac{1}{2}$, $c_6 = 1 - c_3$, $c_7 = 1 - c_2$, $c_8 = 1$, $b_6 = b_3$, $b_7 = b_2$, and $b_8 = b_1$. Vectors \mathbf{x} and \mathbf{y} of 8 components are going to be called “even” and “odd” if $x_6 = x_3$, $x_7 = x_2$, $x_8 = x_1$, and $y_1 + y_8 = y_2 + y_7 = y_3 + y_6 = y_4 = y_5 = 0$, respectively. Let $\mathbf{p}_1 = 2\mathbf{c} - \mathbf{1}$, $\mathbf{p}_2 = 6\mathbf{c}^2 - 6\mathbf{c} + \mathbf{1}$, and $\mathbf{p}_3 = 20\mathbf{c}^3 - 30\mathbf{c}^2 + 12\mathbf{c} - \mathbf{1}$ be the analogs of shifted Legendre polynomials, orthogonal on $[0, 1]$ (see, e.g., (Butcher, 2016, s. 342), (Butcher, 2021, p. 203)). The vectors $\mathbf{1}$, \mathbf{b}^T , and \mathbf{p}_2 are “even”; while \mathbf{p}_1 and \mathbf{p}_3 are “odd”. With such a definition of “even” and “odd” vectors, the eq. (1) could be viewed as the transfiguration of the statements

- if \mathbf{u} is “odd”, then $\mathbf{A}\mathbf{u}$ is “even”
- if \mathbf{u} is “even” and $b\mathbf{u} = 0$, then $\mathbf{A}\mathbf{u}$ is “odd”

To imitate these parity properties, it will be demanded that \mathbf{Ap}_1 is “even” (this implies that the vector $\mathbf{q}_1 = \mathbf{Ac} - \frac{1}{2}\mathbf{c}^2 = \frac{1}{2}\mathbf{Ap}_1 + \frac{1}{2}\mathbf{c}(\mathbf{1} - \mathbf{c})$ is “even” too), and that \mathbf{Ap}_2 and \mathbf{Aq}_1 are “odd”. These demands can be viewed as simplifying assumptions, as they increase the redundancy in the order conditions (for example, the statements $\mathbf{b}\mathbf{1} = 1$ and $\mathbf{b}\mathbf{p}_2 = \mathbf{b}\mathbf{q}_1 = 0$ imply that a method is of order 4). Also the properties $\mathbf{D}(\mathbf{1})$ and $\mathbf{D}(\mathbf{c})$ (or an easier to exploit $\mathbf{D}(\mathbf{p}_1)$) will be assumed.⁵

The vectors $\mathbf{p}_3 - \mathbf{p}_1$, $\mathbf{p}_1 \cdot \mathbf{q}_1$, \mathbf{Ap}_2 , and \mathbf{Aq}_1 are “odd” and have the 1st and the 8th components being equal to 0. Thus, they lie in the span of two vectors: $\mathbf{v}_2 = [0 \ 1 \ 0 \ 0 \ 0 \ 0 \ -1 \ 0]^T$ and $\mathbf{v}_3 = [0 \ 0 \ 1 \ 0 \ 0 \ -1 \ 0 \ 0]^T$. To satisfy the order conditions $\mathbf{D}(\Phi(t_1), \Phi(t_2))$ with $|t_1| = |t_2| = 4$, it is necessary and sufficient that $\mathbf{b}(\mathbf{v}_2 \cdot (\mathbf{Av}_2)) = -a_{72}b_2 = 0$, $\mathbf{b}(\mathbf{v}_3 \cdot (\mathbf{Av}_3)) = -a_{63}b_3 = 0$, and $\mathbf{b}(\mathbf{v}_2 \cdot (\mathbf{Av}_3)) + \mathbf{b}(\mathbf{Av}_2) \cdot \mathbf{v}_3 = (a_{76} - a_{73})b_2 + (a_{32} - a_{62})b_3 = 0$. To support the observance of the parity properties and not to lose the flexibility in choosing b_2 and b_3 , let $a_{63} = a_{72} = 0$, $a_{62} = a_{32}$, and $a_{76} = a_{73}$.

The conditions $-c_2 = (\mathbf{Ap}_1)_2 = (\mathbf{Ap}_1)_7 = -a_{71}$ and $(\mathbf{Ap}_1)_3 = (\mathbf{Ap}_1)_6$ imply $a_{71} = c_2$ and $a_{61} = a_{31}$, respectively. The property $\mathbf{D}_1(\mathbf{p}_1)$ becomes $a_{81}b_1 = 0$, thus $a_{81} = 0$.

The property $\mathbf{D}_2(\mathbf{p}_1)$ implies $a_{82} = c_2b_2/b_1$. Both $\mathbf{D}_7(\mathbf{1})$ and $\mathbf{D}_7(\mathbf{p}_1)$ imply $a_{87} = c_2b_2/b_1$. Now all three $\mathbf{D}_3(\mathbf{p}_1) \Leftrightarrow \mathbf{D}_6(\mathbf{p}_1)$, $\mathbf{D}_8(\mathbf{p}_1)$, and $(\mathbf{Ap}_1)_8 = 0$ imply $a_{86} = a_{83}$.

If $b_2 = 0$, then $\mathbf{D}_6(\mathbf{1})$ implies $a_{83} = c_3b_3/b_1$, and then $\mathbf{D}_6(\mathbf{p}_1)$ means $b_3a_{32}c_2 = 0$. Both cases $b_3 = 0$ and $a_{32} = 0$ lead to contradictions, thus $b_2 \neq 0$. With $a_{31} = c_3 - a_{32}$, the properties $\mathbf{D}_6(\mathbf{1})$ and $\mathbf{D}_6(\mathbf{p}_1)$ imply $a_{83} = a_{31}b_3/b_1$ and $a_{73} = a_{32}b_3/b_2$. The Butcher tableau (Butcher, 1964b, p. 191) now looks like

0								
c_2	c_2							
c_3	a_{31}	a_{32}						
$\frac{1}{2}$	a_{41}	a_{42}	a_{43}					
$\frac{1}{2}$	a_{51}	a_{52}	a_{53}	a_{54}				
$1 - c_3$	a_{31}	a_{32}	0	a_{64}	a_{65}			
$1 - c_2$	c_2	0	$a_{32}\frac{b_3}{b_2}$	a_{74}	a_{75}	$a_{32}\frac{b_3}{b_2}$		
1	0	$c_2\frac{b_2}{b_1}$	$a_{31}\frac{b_3}{b_1}$	a_{84}	a_{85}	$a_{31}\frac{b_3}{b_1}$	$c_2\frac{b_2}{b_1}$	
	b_1	b_2	b_3	b_4	b_5	b_3	b_2	b_1

As $(\mathbf{A1})_6 = 1 - c_3$, let $a_{64} = 1 - 2c_3 - a_{65}$. Then $(\mathbf{Ap}_2)_3 + (\mathbf{Ap}_2)_6 = 0$ implies $c_3 \neq \frac{1}{6}$ and $a_{32} = (6c_3 - 1)/24c_2(1 - c_2)$. As $(\mathbf{A1})_4 = \frac{1}{2}$, let $a_{41} = \frac{1}{2} - a_{42} - a_{43}$. Then $(\mathbf{Ap}_2)_4 = 0$ implies $a_{42} = (1 - 12a_{43}c_3(1 - c_3))/12c_2(1 - c_2)$. Now $(\mathbf{Aq}_1)_4 = 0$ is equivalent to $a_{43} = c_2/(6c_3 - 12c_3(c_3 - c_2) - 1)$, with the denominator necessarily being non-zero. As $(\mathbf{A1})_5 = \frac{1}{2}$, let $a_{51} = \frac{1}{2} - a_{52} - a_{53} - a_{54}$. Then $(\mathbf{Ap}_2)_5 = 0$ implies $a_{54} = \frac{1}{3} - 4a_{52}c_2(1 - c_2) - 4a_{53}c_3(1 - c_3)$.

As $(\mathbf{A1})_7 = 1 - c_2$, let $a_{74} = 1 - 2c_2 - a_{75} - b_3(6c_3 - 1)/12b_2c_2(1 - c_2)$. Then $(\mathbf{Ap}_2)_2 + (\mathbf{Ap}_2)_7 = (b_3(6c_3 - 1)(1 - 2c_3)^2 - 4b_2c_2(1 - c_2)(1 - 6c_2))/8b_2c_2(1 -$

⁵ The derivation was done in interaction with computer algebra system Wolfram Mathematica 8.0, mainly using commands **Solve** to symbolically solve linear equations, **Simplify**, and **Factor**. Step-by-step description of the process (of course, this could be done in many ways) allows for an easy reproduction (also see Appendix).

$c_2) = 0$, thus $b_3 = 4b_2c_2(1 - c_2)(1 - 6c_2)/(1 - 2c_3)^2(6c_3 - 1)$. The coefficient a_{84} is determined from $(\mathbf{A}\mathbf{1})_8 = 1$. Then the derivative of $b_1(\mathbf{A}\mathbf{p}_2)_8$ with respect to b_1 is equal to $-\frac{1}{2} \neq 0$, so $(\mathbf{A}\mathbf{p}_2)_8 = 0$ determines $b_1 = b_2(1 - 12c_2 + 24c_2^2(1 - c_2) - 6c_3 + 96c_2c_3 - 312c_2^2c_3 + 288c_2^3c_3)/(6c_3 - 1)$. Now $\mathbf{A}\mathbf{p}_2 = [0 \ c_2 \ \frac{1-2c_3}{4} \ 0 \ 0 \ -\frac{1-2c_3}{4} \ -c_2 \ 0]^T$ is “odd”, also \mathbf{q}_1 is “even”. The coefficient a_{85} and the weight b_4 are determined from $D_5(\mathbf{1})$ and $\mathbf{b}\mathbf{1} = 1$, respectively.

Now $\mathbf{b}\mathbf{c}^2 = \frac{1}{4} + 2b_2c_2(18c_3(1 - 2c_2)^2 - 1 - 2c_2)/(6c_3 - 1)$. Thus, $18c_3(1 - 2c_2)^2 - 1 - 2c_2 \neq 0$ and $b_2 = (6c_3 - 1)/24c_2(18c_3(1 - 2c_2)^2 - 1 - 2c_2)$.

The coefficient a_{75} is determined from $D_5(\mathbf{p}_1)$.

The properties $D_2(\mathbf{1})$, $D_3(\mathbf{1})$, and $(\mathbf{A}\mathbf{q}_1)_5 = 0$ can be written as $b_5a_{52} + \phi_{2b}b_5 = \phi_{20}$, $b_5a_{53} + \phi_{3b}b_5 = \phi_{30}$, and $\phi_2a_{52} + \phi_3a_{53} = \phi_0$, respectively, where all the coefficients ϕ_{2b} , ϕ_{20} , ϕ_{3b} , ϕ_{30} , ϕ_2 , ϕ_3 , and ϕ_0 are rational functions of c_2 and c_3 . It can be checked that $\phi_2\phi_{2b} + \phi_3\phi_{3b} + \phi_0 = 0$. The following quantity should be equal to zero: $\phi_2(b_5a_{52} + \phi_{2b}b_5 - \phi_{20}) + \phi_3(b_5a_{53} + \phi_{3b}b_5 - \phi_{30}) = b_5(\phi_2a_{52} + \phi_3a_{53} + \phi_2\phi_{2b} + \phi_3\phi_{3b}) - \phi_2\phi_{20} - \phi_3\phi_{30} = b_5(\phi_0 + (-\phi_0)) - \phi_2\phi_{20} - \phi_3\phi_{30} = -(\phi_2\phi_{20} + \phi_3\phi_{30})$. This can be rewritten as

$$\zeta(c_2, c_3) = \sum_{m,n} \zeta_{mn} c_2^m (2c_3)^n = 0$$

5	9	-9			
4	-21	-15	-108	216	
3	15	75	294	-576	
2	-1	-93	-198	396	72
n = 1	-3	53	18	-132	
n = 0	1	-13	20		
ζ_{mn}	m = 0	m = 1	2	3	4

Both coefficients ϕ_{20} and ϕ_{30} are equal to zero at the point $(c_2, c_3) = \mathbf{C} = (2\gamma, 4\gamma)$, where $\gamma = (2 + 2^{1/3} + 2^{-1/3})/12 = 1/4(2 - 2^{1/3}) = 0.33780\dots$. There $\phi_{2b} = 0$ and $\phi_{3b} = 2\gamma - \frac{1}{2}$, thus $a_{53} = \frac{1}{2}(-5 + 48\gamma - 96\gamma^2)a_{52} + \frac{1}{2} - 2\gamma$, also $b_5a_{52} = 0$ (from $D_2(\mathbf{1})$) and $a_{65}a_{52} = 0$ (from $(\mathbf{A}\mathbf{q}_1)_3 + (\mathbf{A}\mathbf{q}_1)_6 = 0$). In both cases of $a_{52} = 0$ (then $\mathbf{a}_{4*} = \mathbf{a}_{5*}$, i.e., the 4th and the 5th stages duplicate each other) and $a_{52} \neq 0$ (then $b_5 = 0$ and $\mathbf{a}_{*5} = \mathbf{0}$, i.e., the 5th stage is not used), the method becomes equivalent to

0							
2γ	2γ						
4γ	0	4γ					
$\frac{1}{2}$	2γ	0	$\frac{1}{2} - 2\gamma$				
1 - 4γ	0	4γ	0	1 - 8γ			
1 - 2γ	2γ	0	$\frac{1}{2} - 2\gamma$	0	$\frac{1}{2} - 2\gamma$		
1	0	4γ	0	1 - 8γ	0	4γ	
	γ	2γ	$\frac{1}{4} - \gamma$	$\frac{1}{2} - 4\gamma$	$\frac{1}{4} - \gamma$	2γ	γ

(2)

This 7-stage pseudo-symplectic Runge–Kutta method of order (4, 9) is strongly connected to a well-known explicit symplectic method for separated Hamiltonians (Forest & Ruth, 1990, eqs. (4.9) and (4.12)), (Yoshida, 1990, eq. (2.11)).

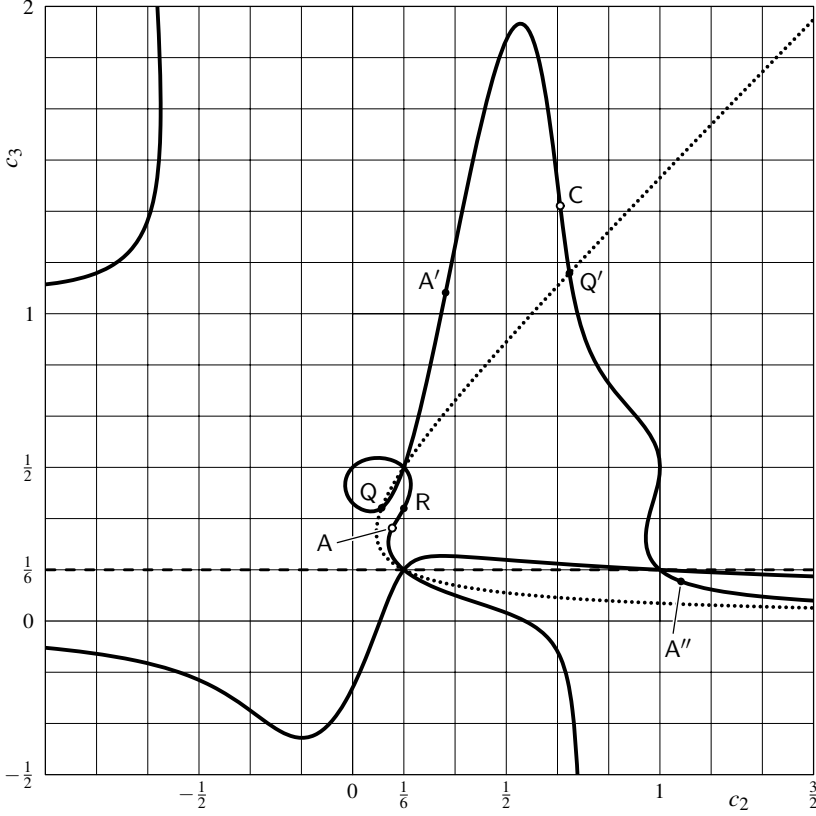


Figure 1 The curve $\zeta(c_2, c_3) = 0$ (solid curve); the line $c_3 = \frac{1}{6}$ (dashed curve); and the hyperbola $6c_3 - 12c_3(c_3 - c_2) - 1 = 0$ (dotted curve, the coefficient a_{43} is infinite on it) which intersects with the curve $\zeta = 0$ at the points $(\frac{1}{6}, \frac{1}{6})$, $(\frac{1}{6}, \frac{1}{2})$, $Q = ((6 - \sqrt{21})/15, (9 - \sqrt{21})/12) = (0.09449\dots, 0.36811\dots)$, and $Q' = ((6 + \sqrt{21})/15, (9 + \sqrt{21})/12) = (0.70550\dots, 1.13188\dots)$. Some branches of the curve $\zeta = 0$ are not shown as they correspond to too large values of c_2 or c_3 to be visible on the graph. The points C and A are indicated by open dots and correspond to the method in eq. (2) and the 1-dimensional family of methods that includes the method in eq. (3), respectively.

Besides the point C one must have $b_5 \neq 0$, and thus $a_{52} = \phi_{20}/b_5 - \phi_{2b}$ and $a_{53} = \phi_{30}/b_5 - \phi_{3b}$. The cubic equation $z(z - \frac{1}{2})(z - 1) = \frac{1}{24}$ has three roots: $z_1 = 1/2 - \sin(2\pi/9)/\sqrt{3} = 0.12888\dots$, $z_2 = 1/2 - \sin(2\pi/9 + 2\pi/3)/\sqrt{3} = 1/8 \sin^2(2\pi/9) = 0.30253\dots$, and $z_3 = 1/2 - \sin(2\pi/9 + 4\pi/3)/\sqrt{3} = 1.06857\dots$. The quantity $b_5((\mathbf{Aq}_1)_3 + (\mathbf{Aq}_1)_6)$, which should be equal to zero, is a linear function of b_5 and a_{65} , and its derivative with respect to b_5 is not equal to zero besides the points $(c_2, c_3) = A = (z_1, z_2)$, $A' = (z_2, z_3)$, and $A'' = (z_3, z_1)$. There the weight b_5 is determined from $(\mathbf{Aq}_1)_3 + (\mathbf{Aq}_1)_6 = 0$, and then a_{65} is found from $(\mathbf{Aq}_1)_8 = 0$. The vector $\mathbf{Aq}_1 = [0 \ 0 \ -\frac{c_2(6c_3-1)}{48(1-c_2)} \ 0 \ 0 \ \frac{c_2(6c_3-1)}{48(1-c_2)} \ 0 \ 0]^T$ is now “odd”. The result is a 1-dimensional (along the curve $\zeta(c_2, c_3) = 0$) family of pseudo-symplectic methods

of order (4, 6) that satisfy $\mathbf{D}(\mathbf{1})$, $\mathbf{D}(\mathbf{c})$, and $\mathbf{D}(\mathbf{c}^2)$, but not $\mathbf{D}(\mathbf{Ac})$. For example, at the point $(c_2, c_3) = \mathbf{R} = (\frac{1}{6}, \frac{11}{30})$ a method is equivalent (the 6th stage is not used) to

0							
$\frac{1}{6}$	$\frac{1}{6}$						
$\frac{11}{30}$	$\frac{1}{150}$	$\frac{9}{25}$					
$\frac{1}{2}$	$\frac{1}{4}$	$-\frac{13}{48}$	$\frac{25}{48}$				
$\frac{1}{2}$	$-\frac{37}{50}$	$\frac{59}{25}$	-2	$\frac{22}{25}$			
$\frac{5}{6}$	$\frac{1}{6}$	0	0	$\frac{4}{11}$	$\frac{10}{33}$		
1	0	$\frac{3}{8}$	0	$\frac{4}{11}$	$-\frac{5}{44}$	$\frac{3}{8}$	
	$\frac{1}{12}$	$\frac{3}{16}$	0	$\frac{4}{11}$	$\frac{25}{264}$	$\frac{3}{16}$	$\frac{1}{12}$

At all the three points \mathbf{A} , \mathbf{A}' , and \mathbf{A}'' the vector \mathbf{Aq}_1 is “odd”, plus $\mathbf{D}(\mathbf{1})$ and $\mathbf{D}(\mathbf{c})$ are satisfied. The coefficient a_{65} is determined from $D_5(\mathbf{c}^2)$. Now $\mathbf{D}(\mathbf{c}^2)$ and $\mathbf{D}(\mathbf{Ac})$ are satisfied, and the result is a 1-dimensional family of 8-stage pseudo-symplectic Runge–Kutta methods of order (4, 8) indexed by a parameter ψ :

0								
c_2	c_2							
c_3	0	c_3						
$\frac{1}{2}$	$\frac{1}{2} - c_2$	$c_2 + c_3 - 1$	$1 - c_3$					
$\frac{1}{2}$	a_{51}	a_{52}	a_{53}	a_{54}				
$1 - c_3$	0	c_3	0	a_{64}	a_{65}			
$1 - c_2$	c_2	0	$\frac{1}{2} - 2c_2$	a_{74}	a_{75}	$\frac{1}{2} - 2c_2$		
1	0	c_3	0	a_{64}	a_{65}	0	c_3	
	$\frac{1}{2}c_2$	$\frac{1}{2}c_3$	$\frac{1}{4} - c_2$	b_4	b_5	$\frac{1}{4} - c_2$	$\frac{1}{2}c_3$	$\frac{1}{2}c_2$

$$\begin{bmatrix} \mathbf{a}_{4*} \\ \mathbf{a}_{5*} \end{bmatrix} = \begin{bmatrix} \varphi c_2 & (1 - \varphi)c_3 & \varphi(\frac{1}{2} - 2c_2) & \varphi c_2 + (1 - \varphi)(\frac{1}{2} - c_3) & 0 & 0 & 0 & 0 \\ \psi c_2 & (1 - \psi)c_3 & \psi(\frac{1}{2} - 2c_2) & \psi c_2 + (1 - \psi)(\frac{1}{2} - c_3) & 0 & 0 & 0 & 0 \end{bmatrix}$$

$$\begin{bmatrix} a_{64} & a_{65} \\ a_{74} & a_{75} \\ b_4 & b_5 \end{bmatrix} = \begin{bmatrix} 2(\frac{1}{2} - c_3)(1 - \chi) & 2(\frac{1}{2} - c_3)\chi \\ 2c_2(1 + \chi) & -2c_2\chi \\ \frac{1}{2}(a_{64} + a_{74}) & \frac{1}{2}(a_{65} + a_{75}) \end{bmatrix}, \quad \chi = \frac{4(1 - 3c_2)}{(1 - 6c_2)(\varphi - \psi)}$$

Here $c_2(c_2 - \frac{1}{2})(c_2 - 1) = \frac{1}{24}$, $c_3 = c_2(1 - c_2)/(\frac{1}{2} - c_2) = 1/6(1 - 2c_2)^2$, and $\varphi = (\frac{1}{2} - c_3)/(\frac{1}{2} - c_2 - c_3) = 1/2c_2 - 1$. Out of these three points, the methods at the point $(c_2, c_3) = \mathbf{A} = (z_1, z_2) = (0.12888\dots, 0.30253\dots)$ are the most efficient.

The residuals in the properties $D(\Phi(t_1), \Phi(t_2))$ with $|t_1| = 4$ and $|t_2| = 5$ are inversely proportional to b_5 . In the limit $b_5 \rightarrow \infty$, or $\psi \rightarrow \varphi$, one gets a method that uses information about the derivative of the r.h.s. function \mathbf{f} (Butcher, 2016,

s. 224), (Hairer & Wanner, 1996, s. IV.7). As the sum $b_4 + b_5$ does not depend on ψ , maximizing b_5 but keeping $b_4 \geq 0$ leads to $b_4 = 0$, $\psi = (\frac{1}{2} - c_3)/(\frac{1}{2} + c_2 - c_3) = 2c_3$:

$$\begin{array}{c|cccccccc}
 0 & & & & & & & & c_2 = \frac{1}{2} - \frac{1}{\sqrt{3}} \sin(\frac{2\pi}{9}) \\
 c_2 & c_2 & & & & & & & c_3 = \frac{1}{2} - \frac{1}{\sqrt{3}} \sin(\frac{\pi}{9}) \\
 c_3 & 0 & c_3 & & & & & & \\
 \frac{1}{2} & \frac{1}{2} - c_2 & c_2 + c_3 - 1 & 1 - c_3 & & & & & \\
 \frac{1}{2} & 2c_2c_3 & (1 - 2c_3)c_3 & (1 - 4c_2)c_3 & 4c_2c_3 & & & & (3) \\
 1 - c_3 & 0 & c_3 & 0 & 4c_2 - 2 & \frac{1}{2c_2} - 2 & & & \\
 1 - c_2 & c_2 & 0 & \frac{1}{2} - 2c_2 & 2 - 4c_2 & 6c_2 - 2 & \frac{1}{2} - 2c_2 & & \\
 1 & 0 & c_3 & 0 & 4c_2 - 2 & \frac{1}{2c_2} - 2 & 0 & c_3 & \\
 \hline
 & \frac{1}{2}c_2 & \frac{1}{2}c_3 & \frac{1}{4} - c_2 & 0 & \frac{1}{2} + c_2 - c_3 & \frac{1}{4} - c_2 & \frac{1}{2}c_3 & \frac{1}{2}c_2
 \end{array}$$

All the nodes, weights, and coefficients are elements of the algebraic extension $\mathbf{Q}(c_2) = \{\alpha_1 + \alpha_2 c_2 + \alpha_3 c_3 \mid \alpha_1, \alpha_2, \alpha_3 \in \mathbf{Q}\}$ of the field of rational numbers \mathbf{Q} . For example, $c_2^2 = -\frac{1}{12} + \frac{7}{6}c_2 - \frac{1}{6}c_3$, $c_2c_3 = -\frac{1}{12} + \frac{1}{6}c_2 + \frac{1}{3}c_3$, $c_3^2 = -\frac{1}{3} + \frac{1}{6}c_2 + \frac{4}{3}c_3$, and $a_{65} = a_{85} = 1/2c_2 - 2 = \varphi - 1 = 3 - 4c_2 - 2c_3$.

The stability function of the method in eq. (3) is equal to

$$R(z) = 1 + z + \frac{1}{2}z^2 + \frac{1}{6}z^3 + \frac{1}{24}z^4 + \frac{1}{120}r_5z^5 + \frac{1}{720}r_6z^6 + \frac{1}{5040}r_7z^7 + \frac{1}{40320}r_8z^8$$

where $r_5 = \frac{5}{6} + \frac{10}{3}c_2 - \frac{5}{6}c_3 = 1.0108\dots$, $r_6 = 20c_2 - 5c_3 = 6r_5 - 5 = 1.0650\dots$, $r_7 = -\frac{35}{8} + 105c_2 - \frac{105}{4}c_3 = 1.2165\dots$, and $r_8 = -\frac{70}{3} + \frac{1400}{3}c_2 - \frac{350}{3}c_3 = 1.5179\dots$

The basic properties of new methods eq. (2), eq. (3) and of some known Runge–Kutta methods are compared in Figure 2 and in Table 1, where (and also in Figures 4 and 5) the latter methods are named as follows: RK4 is the classical Runge–Kutta method (Kutta, 1901, p. 448); AC36 is (Aubry & Chartier, 1998a, fig. 4.1);⁶ CLMR47 is (Calvo *et al.*, 2010, p. 262);⁷ CCRL47 is (Capuano *et al.*, 2017, p. 90); CV8 is (Cooper & Verner, 1972, tab. 1), (Butcher, 2016, p. 210); and GL4 is the 2-stage Gauss–Legendre method (Hammer & Hollingsworth, 1955), (Butcher, 1964a, p. 56).

3 Numerical tests

In this section the Runge–Kutta methods from Table 1 are tested on three numerical examples: torque-free rotation of a rigid body (Landau & Lifshitz, 1976, s. 36), a pendulum with a non-separable Hamiltonian (Hairer *et al.*, 1993, ex. 16.2, p. 313), and a periodic Toda lattice (Toda, 1967).

⁶ In (Aubry & Chartier, 1998a, p. 453) it is stated that a certain optimization over methods satisfying $\hat{D}([\tau])$ (same as property $\mathbf{D}(\mathbf{c})$) results in $c_2 = 0.000050587\dots$. Nevertheless, optimization over methods not necessarily satisfying $\hat{D}([\tau])$ led to the method (Aubry & Chartier, 1998a, fig. 4.1) that satisfies $\hat{D}([\tau])$ and has $c_2 = 0.13502\dots$

⁷ In (Calvo *et al.*, 2010, p. 262) the denominators “355,568”, “831,328”, and “9,955,904” in a_{42} , a_{51} , and a_{62} should be read as “3,555,680”, “8,313,280”, and “99,559,040”, respectively.

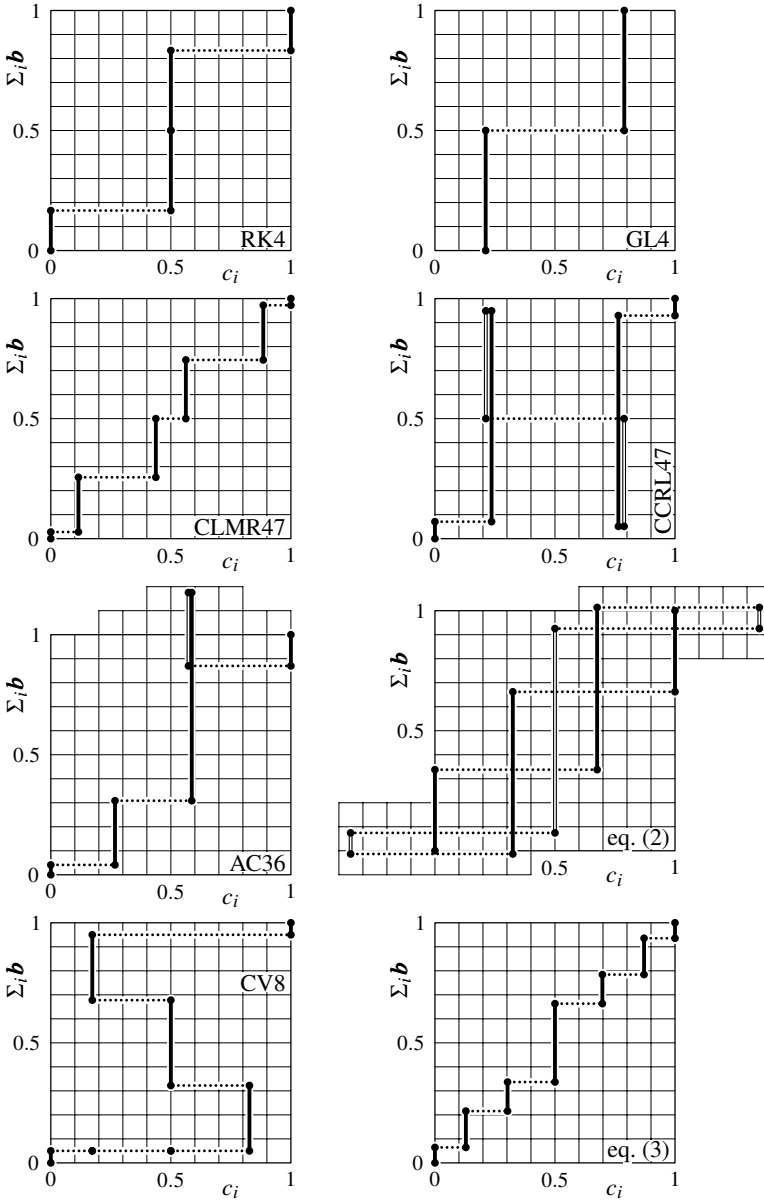


Figure 2 Quadrature scheme graphical depiction (see also (Suzuki, 1990, fig. 1), where the vertical coordinate is the stage) for the eight methods listed in Table 1. Here $\Sigma_i \mathbf{b} = \sum_{j=1}^i b_j$, where $1 \leq i \leq s$, are the cumulative weights, with $\Sigma_0 \mathbf{b} = 0$. Due to the order condition $\mathbf{b} \mathbf{1} = 1$ for an s -stage method one has $\Sigma_s \mathbf{b} = 1$. On the diagram the points $(c_i, \Sigma_{i-1} \mathbf{b})$ and $(c_i, \Sigma_i \mathbf{b})$, where $1 \leq i \leq s$, are connected by a thick line (with white filling if $\Sigma_i \mathbf{b} < \Sigma_{i-1} \mathbf{b}$). To easier follow the progression of the stages, the points $(c_i, \Sigma_i \mathbf{b})$ and $(c_{i+1}, \Sigma_i \mathbf{b})$, where $1 \leq i < s$, are connected by dotted lines.

	s	p	q	$10^4 \times T_4$	$10^3 \times T_5$	$10^3 \times T_6$	$R(z)R(-z) - 1$
RK4	4	4	4	0	14.504...	16.035...	$0.01388888... z^6$
AC36	5	3	6	7.5690...	2.3451...	3.9611...	$-0.00057870... z^8$
CLMR47	6	4	7	0	0.29185...	0.39787...	$0.00024760... z^8$
CCRL47	6	4	7	0	1.4813...	1.6278...	$-0.00030365... z^8$
eq. (2)	7	4	9	0	112.99...	132.54...	$-0.00144678... z^{10}$
eq. (3)	8	4	8	0	0.64048...	0.91796...	$0.00000950... z^{10}$
CV8	11	8	8	0	0	0	$0.00000627... z^{10}$
GL4	2	4	∞	0	4.3306...	5.6178...	0
	$C(2)$	$D(1)$	$D(c)$	$D(c^2)$	$D(Ac)$	$\max_{ij} a_{ij} $	$\min_j b_j$
RK4	F	T	F	F	F	1	0.1666...
AC36	F	T	T	F	F	2.1621...	-0.3054...
CLMR47	F	T	T	T	T	4.4309...	0.0277...
CCRL47	F	T	T	T	T	2.9265...	-0.4488...
eq. (2)	F	T	T	T	T	1.7024...	-0.8512...
eq. (3)	F	T	T	T	T	1.8793...	0.0644...
CV8	T	T	F	F	F	14.728...	0.05
GL4	T	T	T	T	T	0.5386...	0.5

Table 1 A comparison of eight s -stage Runge–Kutta methods of order (p, q) . Error coefficients are defined as $T_p^t = \sum_{t, |t|=p} (\mathbf{b}\Phi(\mathbf{t}) - 1/t!)^2 / \sigma^2(\mathbf{t}) = (1/p!)^2 \sum_{t, |t|=p} \alpha^2(\mathbf{t}) (t! \mathbf{b}\Phi(\mathbf{t}) - 1)^2$, where $\sigma(\mathbf{t})$ is the order of the symmetry group of the tree \mathbf{t} , and $\alpha(\mathbf{t})$ is the number of monotonic labelings of \mathbf{t} (see, e.g., (Butcher, 2016, ss. 304 and 318), (Hairer et al., 1993, pp. 147 and 158), (Butcher, 2021, pp. 58 and 60), (Hairer et al., 2006, pp. 57 and 58)). The column about the function $R(z)R(-z) - 1$ shows the first non-zero term in its Taylor expansion about $z = 0$. Within the 1-dimensional families of methods at the points A, A', and A'' the error coefficients T_5, T_6 , and the stability function $R(z)$ do not depend on the parameter ψ . The symbols T/F stand for true/false. The explicit version of the property C(2) is used. The $\min_j b_j$ column shows the minimal value of a non-zero weight.

Euler's equations describing free rotation of a rigid body with principal moments of inertia $I_1 = 1$, $I_2 = 2$, and $I_3 = 3$ are $d\omega_1/dt = -\omega_2\omega_3$, $d\omega_2/dt = \omega_1\omega_3$, and $d\omega_3/dt = -\frac{1}{3}\omega_1\omega_2$. The solution with initial condition $(\omega_1, \omega_2, \omega_3)|_{t=0} = (12, 0, 7)$ is shown in Figure 3. The pair of quadratic invariants, twice the kinetic energy $2T = I_1\omega_1^2 + I_2\omega_2^2 + I_3\omega_3^2 = 291$ and squared magnitude of the angular momentum $L^2 = I_1^2\omega_1^2 + I_2^2\omega_2^2 + I_3^2\omega_3^2 = 585$, can be reduced to $Q_1(\boldsymbol{\omega}) = \omega_1^2 + \omega_2^2 = 144$ and $Q_2(\boldsymbol{\omega}) = \omega_2^2 + 3\omega_3^2 = 147$. When this system of differential equations is solved numerically, the values of the invariants Q_1 and Q_2 gradually drift from their initial values 144 and 147, see Figure 4. Due to round-off errors, $Q_1(\tilde{\boldsymbol{\omega}}(nh))$ and $Q_2(\tilde{\boldsymbol{\omega}}(nh))$ as functions of n can be approximately viewed as random walks. In the absence of a systematic drift the typical deviation of (Q_1, Q_2) from (144, 147) grows roughly proportional to \sqrt{n} , e.g., the slope of the curves near the bottom of Figure 4, where the round-off errors dominate, is about $\frac{1}{2}$. Even a small bias makes the deviation to eventually, i.e., for large enough n , be proportional to n : in the log-log plots of Figure 4 the slopes of most of the curves are equal to 1. The performances of AC36, CLMR47, and CCRL47 methods are close, with AC36 doing the best out of the three. Besides the implicit GL4, the methods in eq. (2) and eq. (3), and also CV8, due to their higher pseudo-symplecticity order have the fastest rate of decrease of the error in Q_1 and Q_2 with the step size h (see the two right panels in Figure 4). The method in eq. (3), out of the explicit methods tested, has the best performance.

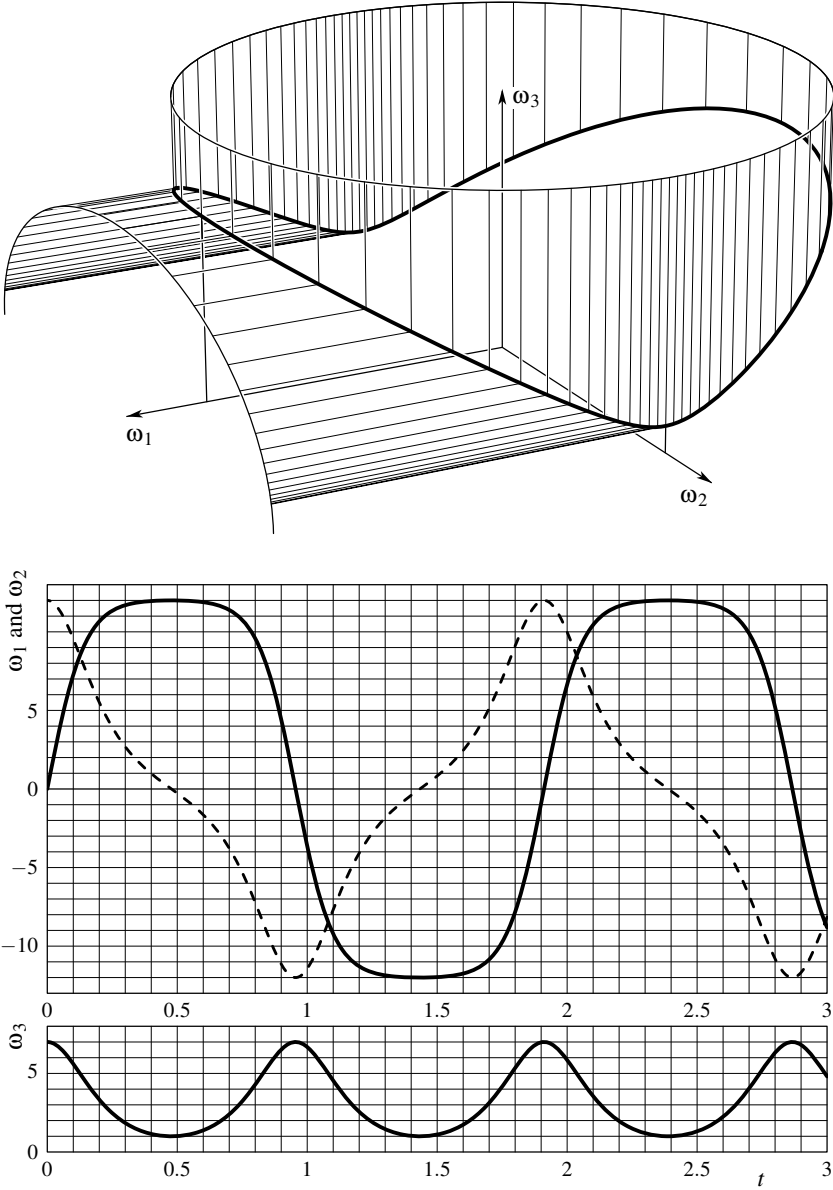


Figure 3 A solution of Euler's equations with moments of inertia $I_1 = 1$, $I_2 = 2$, and $I_3 = 3$: $(\omega_1, \omega_2, \omega_3)(t) = (12\text{cn}, 12\text{sn}, 7\text{dn})\left(7t, \frac{48}{49}\right)$, where cn , sn , and dn are the Jacobi elliptic functions. The motion is periodic with the period $4K\left(\frac{48}{49}\right)/7 = 1.9109\dots$, where $K(m) = \int_0^{\pi/2} d\theta / (1 - m \sin^2 \theta)^{1/2}$ is the complete elliptic integral of the 1st kind. The circular and elliptic cylinders correspond to the quadratic invariants $Q_1(\boldsymbol{\omega}) = \omega_1^2 + \omega_2^2 = 144$ and $Q_2(\boldsymbol{\omega}) = \omega_2^2 + 3\omega_3^2 = 147$, respectively. The thin lines on them divide the period into 72 equal parts. Points of the trajectory that are connected by vertical lines with ω_1 and ω_2 axes are $(12, 0, 7)$ and $(0, 12, 1)$. The alternating behavior of $\omega_2(t)$ is due to the rotation around the intermediate principal axis being unstable (Poinsot, 1834, p. 48), (Landau & Lifshitz, 1976, s. 37).

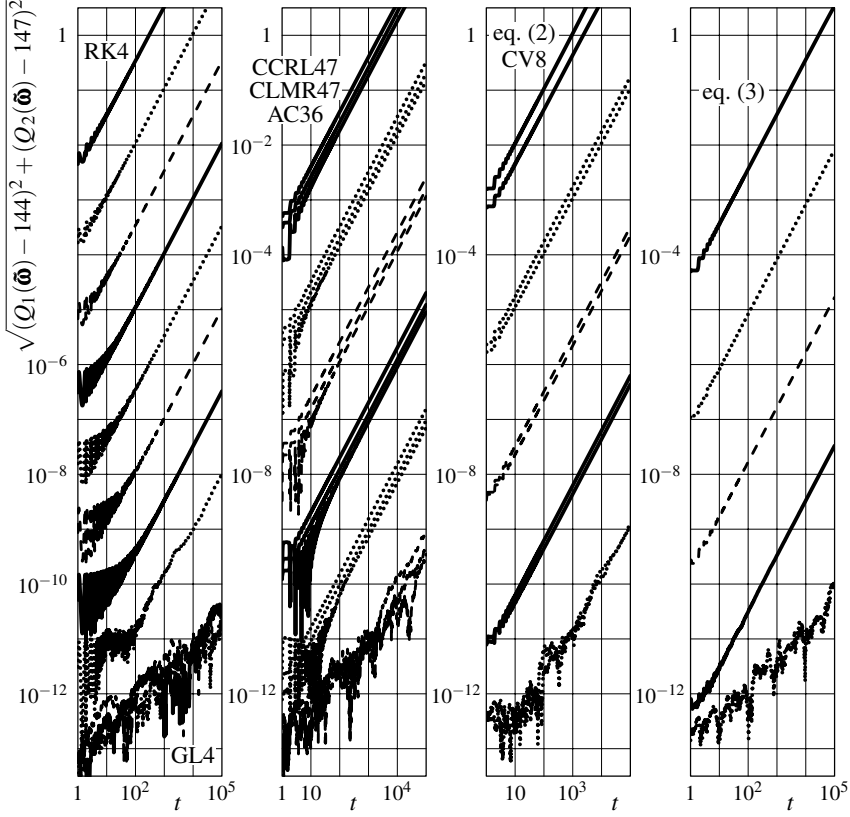


Figure 4 Growth of the error in $Q_1(\tilde{\omega})$ and $Q_2(\tilde{\omega})$ with time t . Panels from left to right: (1) RK4 (curves from top to near bottom) and GL4 (bottom curves); (2) AC36 (lower curves in groups of three), CLMR47 (middle curves), and CCRL47 (upper curves); (3) CV8 and eq. (2) (lower and upper curves in pairs); and (4) eq. (3). The step size is $h = sh_1$, where s is the number of stages. Upper solid, dotted, and dashed curves correspond to $h_1 = 2^{-7}$, $h_1 = 2^{-8}$, and $h_1 = 2^{-9}$, respectively. Next to upper solid or dotted curves correspond to $h_1 = 2^{-10}$ or $h_1 = 2^{-11}$, respectively, and so on, i.e., going to the next, with a different line style, curve down divides h_1 by 2. Upper solid curves, upper dotted curves, and so on, on different panels correspond to the same value of h_1 , and thus to the same number of the r.h.s. function $f(t, x)$ evaluations.

The 2nd numerical example is a system $dx/dt = \partial \mathcal{H} / \partial p$, $dp/dt = -\partial \mathcal{H} / \partial x$, with the Hamiltonian function $\mathcal{H}(p, x) = \frac{1}{2}p^2 - (1 - \frac{1}{6}p)\cos(x)$. The solution with initial condition $(x, p)|_{t=0} = (\arccos(-0.8), 0)$ forms a periodic trajectory along the closed level curve $\mathcal{H}(p, x) = 0.8$ around the origin. Because of notable variations of the Hamiltonian within a period in a numerical solution (see, e.g., Figure 6), here the speed of the systematic drift of the Hamiltonian \mathcal{H} is estimated through the difference between weighted moving average values at two different moments of time. For the eight methods in Table 1, how the drift of the Hamiltonian depends on the step size h , is shown in Figure 5. Again, the performances of AC36, CLMR47, and CCRL47 methods are close, with AC36 doing the best out of the three. In the triple of higher order explicit methods, the ones in eq. (2) and eq. (3) outperform CV8.⁸

⁸ Although with the same amount of work the drift of the Hamiltonian for CV8 is about 15 times faster than for the method in eq. (3), the course of trajectory $(x(t), p(t))$ within a period is computed more accurately by the 8th order method CV8.

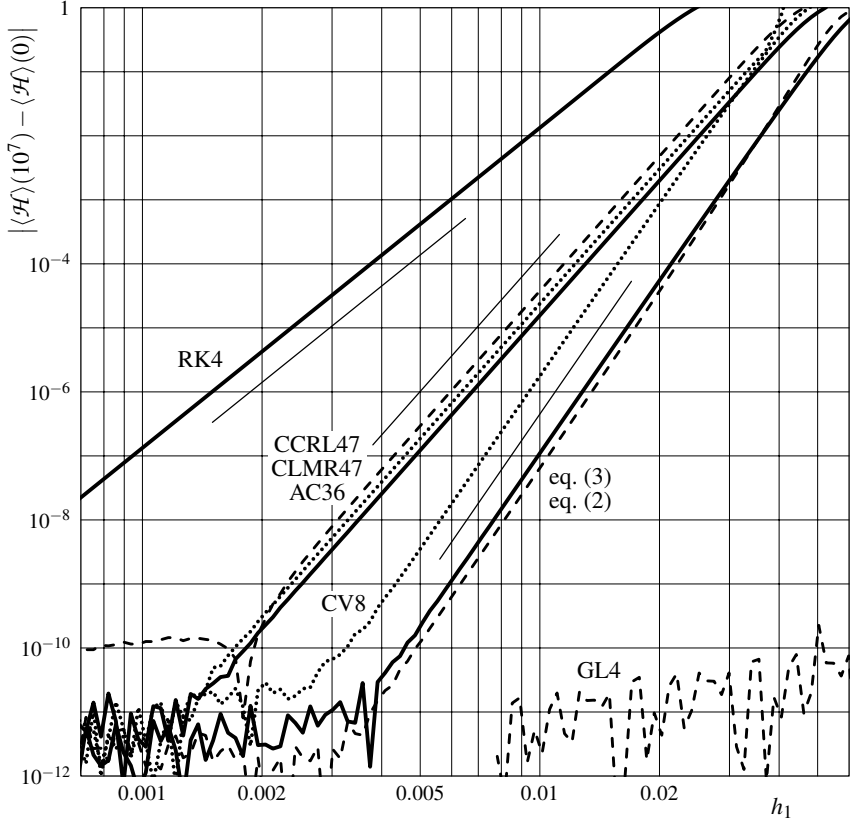


Figure 5 The speed of the systematic drift of the Hamiltonian \mathcal{H} as the function of the step size $h = sh_1$, where s is the number of stages. The number of the r.h.s. function $f(t, \mathbf{x})$ evaluations is equal to the time duration of the simulation (which is 10020000 here) divided by h_1 , and with h_1 being fixed is independent of the method. The curves correspond to RK4, AC36, and eq. (3) (solid curves from top to bottom), CLMR47 and CV8 (upper and lower dotted curves), and CCRL47, eq. (2), and GL4 (dashed curves from top to bottom). Three thin solid lines on this log-log plot have slopes 5, 7, and 9, which corresponds to the speed of the drift being proportional to h^5 , h^7 , and h^9 . The weighted moving average of the Hamiltonian that was used is $\langle \mathcal{H} \rangle(t) = \sum_{n \in \mathcal{S}(t)} \sin^2(\pi(nh - t)/20000) \mathcal{H}(\bar{p}(nh), \bar{x}(nh)) / \sum_{n \in \mathcal{S}(t)} \sin^2(\pi(nh - t)/20000)$, where $\mathcal{S}(t) = \{n \mid t < nh < t + 20000\}$. The simulations were run at the University of Arizona High Performance Computing center.

The 3rd numerical example is the periodic Toda lattice with $N = 32$ nodes:

$$\mathcal{H}(\mathbf{p}, \mathbf{x}) = \frac{1}{2} \sum_{n=1}^N p_n^2 + \sum_{n=1}^N U(x_n - x_{n-1}), \quad U(r) = \exp(-r) + r - 1$$

$$\frac{dx_n}{dt} = \frac{\partial \mathcal{H}}{\partial p_n} = p_n, \quad \frac{d^2 x_n}{dt^2} = \frac{dp_n}{dt} = -\frac{\partial \mathcal{H}}{\partial x_n} = \exp(x_{n-1} - x_n) - \exp(x_n - x_{n+1})$$

with the periodicity condition $x_0 \equiv x_N$. This Hamiltonian system is completely integrable and can be reformulated as the Lax equation $d\mathbf{L}/dt = [\mathbf{L}, \mathbf{A}] = \mathbf{L}\mathbf{A} - \mathbf{A}\mathbf{L}$, with

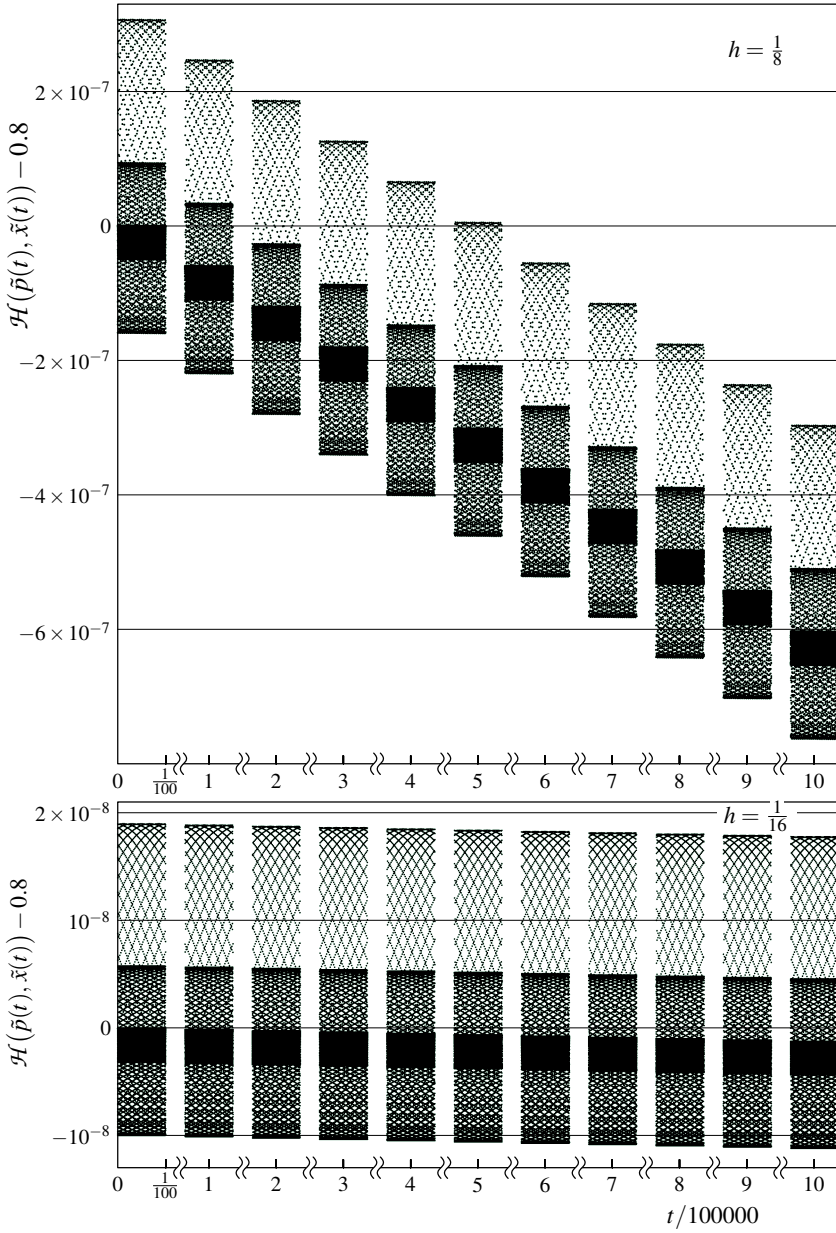


Figure 6 The Hamiltonian $\mathcal{H}(\tilde{p}(t), \tilde{x}(t))$ computed on the numerical solution obtained by the method in eq. (3). The vertical scale in the lower panel (time step $h = \frac{1}{16}$) is 16 times larger than in the upper one ($h = \frac{1}{8}$). Similarity of heights of the depicted Hamiltonian deviations in the two panels is the consequence of the method being of order 4. In order to show both the deviations small time scale structure and the systematic drift of the Hamiltonian, from the whole simulation (which lasts 1000500) eleven fragments of duration 1000 are shown. As the method conserves the symplectic structure up to the order 8, the speed of the systematic drift decreases with h much faster than the magnitude of the deviations within a period.

the Lax pair

$$\mathbf{L} = \begin{bmatrix} b_1 & a_1 & 0 & 0 & \cdots & 0 & a_N \\ a_1 & b_2 & a_2 & 0 & \cdots & 0 & 0 \\ 0 & a_2 & b_3 & a_3 & \cdots & 0 & 0 \\ 0 & 0 & a_3 & b_4 & \cdots & 0 & 0 \\ \vdots & \vdots & \vdots & \vdots & \ddots & \vdots & \vdots \\ 0 & 0 & 0 & 0 & \cdots & b_{N-1} & a_{N-1} \\ a_N & 0 & 0 & 0 & \cdots & a_{N-1} & b_N \end{bmatrix}, \quad \mathbf{A} = \begin{bmatrix} 0 & -a_1 & 0 & 0 & \cdots & 0 & a_N \\ a_1 & 0 & -a_2 & 0 & \cdots & 0 & 0 \\ 0 & a_2 & 0 & -a_3 & \cdots & 0 & 0 \\ 0 & 0 & a_3 & 0 & \cdots & 0 & 0 \\ \vdots & \vdots & \vdots & \vdots & \ddots & \vdots & \vdots \\ 0 & 0 & 0 & 0 & \cdots & 0 & -a_{N-1} \\ -a_N & 0 & 0 & 0 & \cdots & a_{N-1} & 0 \end{bmatrix}$$

where $a_n = \frac{1}{2} \exp(\frac{1}{2}(x_{n-1} - x_n))$, $b_n = -\frac{1}{2}p_{n-1}$ are the so-called Flaschka variables (Flaschka, 1974). Due to periodicity, $p_0 \equiv p_N$ and $b_1 = -\frac{1}{2}p_N$. All N eigenvalues $\lambda_1, \lambda_2, \dots, \lambda_N$ of \mathbf{L} are integrals of motion (Lax, 1968). The coefficients of the characteristic polynomial $\det(\lambda \mathbf{I} - \mathbf{L})$ are related to the integrals of motion found in (Hénon, 1974), see (Flaschka, 1974) for details. In particular, the total momentum $P = \sum_{n=1}^N p_n = -2\text{tr} \mathbf{L} = -2\sum_{n=1}^N \lambda_n$ and the Hamiltonian $\mathcal{H} = 2\text{tr} \mathbf{L}^2 - N = 2\sum_{n=1}^N \lambda_n^2 - N$ do not depend on time.

The initial condition $x_n(0) = 0$ for all $1 \leq n \leq N$, $p_n(0) = 0$ for all $1 \leq n < N$, and $p_N(0) = 1$ was used in the simulations. It corresponds to $P = 1$, $\mathcal{H} = \frac{1}{2}$, $a_n(0) = \frac{1}{2}$ for all $1 \leq n \leq N$, $b_n(0) = 0$ for all $1 \leq n < N$, and $b_N(0) = -\frac{1}{2}$. The whole system is in equilibrium and at rest, with the exception of the N^{th} particle which moves with velocity $p_N(0) = 1$. The evolution of the system over the time interval $0 \leq t \leq 60$ is shown in Figure 7.

How the systematic drift of the integrals of motion λ_n , $1 \leq n \leq 32$, depends on the step size h , is shown in Figure 8. The performances of AC36, CLMR47, and CCRL47 methods are close, with AC36 doing the best out of the three, the CLMR47 and CCRL47 curves are omitted. The CLMR47 and eq. (2) methods are prone to cause numerical overflow at large time steps h , most probably due to the presence of exponential function in the r.h.s. The method in eq. (3) is capable of conserving up to the 8th order multiple integrals of motion that are far from being quadratic, with a bit better performance than CV8 for the same amount of r.h.s. function evaluations.

Conclusions

There are known 5- and 6-stage pseudo-symplectic Runge–Kutta methods of order (3, 6) and (4, 7), respectively, see, e.g., Table 1. With 7 stages it is possible to come up with a method of order (4, 9), see eq. (2). Utilising 8 stages, one can construct robust, with non-negative weights and monotonically increasing nodes, methods of order (4, 8), see eq. (3). The newly derived methods, largely due to their higher order, have better quadratic invariants and energy preservation properties than previously known pseudo-symplectic methods.

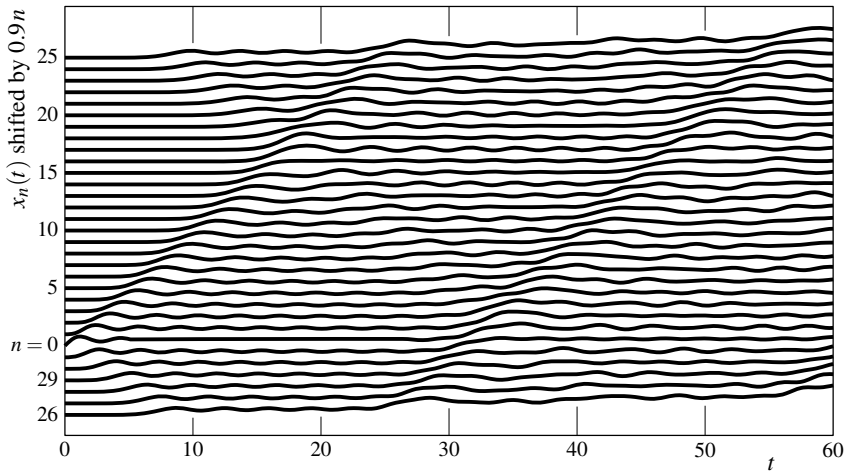


Figure 7 Evolution of the periodic Toda lattice with $N = 32$ and initial condition $x_n(0) = 0$ for all $1 \leq n \leq 32$, $p_n(0) = 0$ for all $1 \leq n < 32$, and $p_0(0) = p_{32}(0) = 1$. To show wave-like perturbations propagating both to the right and to the left from the initial disturbance at $n = 32 \equiv 0$, the curves corresponding to $n \geq 26$ are drawn at the bottom, with n being treated modulo 32. All the curves slowly but systematically climb up, as the total momentum $P = \sum_{n=1}^N p_n(t) = 1$ is positive.

References

- V. I. Arnold, *Mathematical methods of classical mechanics*, 2nd ed., Springer (1989). DOI:10.1007/978-1-4757-2063-1
- U. M. Ascher, L. R. Petzold, *Computer methods for ordinary differential equations and differential-algebraic equations*, SIAM (1998). DOI:10.1137/1.9781611971392
- A. Aubry, P. Chartier, *Pseudo-symplectic Runge–Kutta methods*, BIT **38** (3) 439–461 (1998a). DOI:10.1007/BF02510253
- A. Aubry, P. Chartier, *A note on pseudo-symplectic Runge–Kutta methods*, BIT **38** (4) 802–806 (1998b). DOI:10.1007/BF02510415
- K. Burrage, J. C. Butcher, *Stability criteria for implicit Runge–Kutta methods*, SIAM Journal on Numerical Analysis **16** (1) 46–57 (1979). DOI:10.1137/0716004
- J. C. Butcher, *Implicit Runge–Kutta processes*, Mathematics of Computation **18** (85) 50–64 (1964a). DOI:10.2307/2003405
- J. C. Butcher, *On Runge–Kutta processes of high order*, Journal of the Australian Mathematical Society **4** (2) 179–194 (1964b). DOI:10.1017/S1446788700023387
- J. C. Butcher, *An algebraic theory of integration methods*, Mathematics of Computation **26** (117) 79–106 (1972). DOI:10.1090/S0025-5718-1972-0305608-0
- J. C. Butcher, *A stability property of implicit Runge–Kutta methods*, BIT **15** (4) 358–361 (1975). DOI:10.1007/BF01931672
- J. C. Butcher, *Numerical methods for ordinary differential equations*, 3rd ed., John Wiley & Sons Ltd (2016). DOI:10.1002/9781119121534
- J. C. Butcher, *B-series: algebraic analysis of numerical methods*, Springer (2021). DOI:10.1007/978-3-030-70956-3

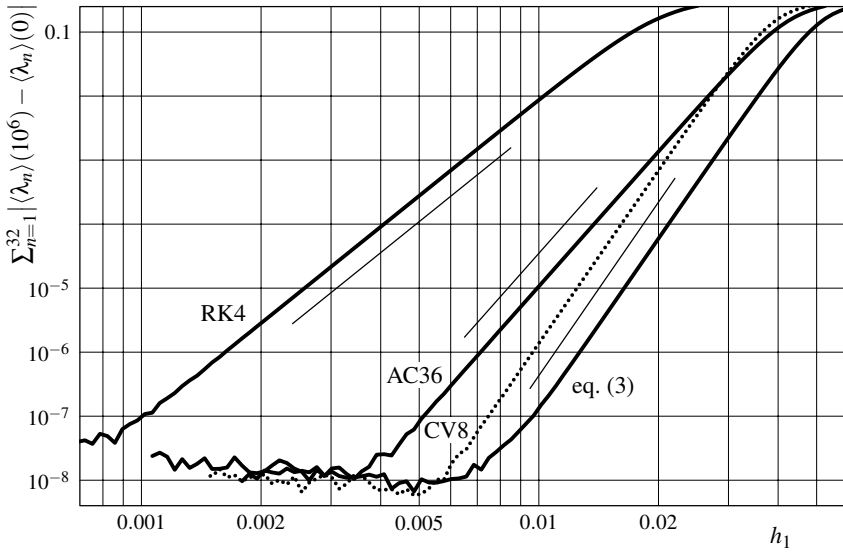


Figure 8 The combined speed of the systematic drift of $N = 32$ integrals of motion λ_n , $1 \leq n \leq 32$, that are the eigenvalues of L as the function of the step size $h = sh_1$, where s is the number of stages. The number of the r.h.s. function $f(t, \mathbf{x})$ evaluations is equal to the time duration of the simulation (which is 1002000 here) divided by h_1 , and with h_1 being fixed is independent of the method. The curves correspond to RK4, AC36, and eq. (3) (solid curves from top to bottom), and CV8 (dotted curve). Three thin solid lines on this log-log plot have slopes 5, 7, and 9, which corresponds to the speed of the drift being proportional to h^5 , h^7 , and h^9 . The weighted moving average that was used is $\langle \lambda \rangle(t) = \sum_{n \in \mathcal{S}(t)} \sin^2(\pi(nh - t)/2000) \lambda(nh) / \sum_{n \in \mathcal{S}(t)} \sin^2(\pi(nh - t)/2000)$, where $\mathcal{S}(t) = \{n \mid t < nh < t + 2000\}$. The simulations were run at the University of Arizona High Performance Computing center.

- J. C. Butcher, G. Wanner, *Runge–Kutta methods: some historical notes*, Applied Numerical Mathematics **22** (1–3) 113–151 (1996). DOI:10.1016/S0168-9274(96)00048-7
- M. Calvo, M. P. Laburta, J. I. Montijano, L. Rández, *Approximate preservation of quadratic first integrals by explicit Runge–Kutta methods*, Advances in Computational Mathematics **32** (3) 255–274 (2010). DOI:10.1007/s10444-008-9105-4
- F. Capuano, G. Coppola, L. Rández, L. de Luca, *Explicit Runge–Kutta schemes for incompressible flow with improved energy-conservation properties*, Journal of Computational Physics **328**, 86–94 (2017). DOI:10.1016/j.jcp.2016.10.040
- A. Cayley, Esq.: XXVIII. *On the theory of the analytical forms called trees*, The London, Edinburgh, and Dublin Philosophical Magazine and Journal of Science **13** (85) 172–176 (1857). DOI:10.1080/14786445708642275
- G. J. Cooper, *Stability of Runge–Kutta methods for trajectory problems*, IMA Journal of Numerical Analysis **7** (1) 1–13 (1987). DOI:10.1093/imanum/7.1.1
- G. J. Cooper, J. H. Verner, *Some explicit Runge–Kutta methods of high order*, SIAM Journal on Numerical Analysis **9** (3) 389–405 (1972). DOI:10.1137/0709037
- P. Cvitanović, *Group theory: birdtracks, Lie’s, and exceptional groups*, Princeton University Press (2008). DOI:10.1515/9781400837670

- P. A. M. Dirac, *A new notation for quantum mechanics*, Mathematical Proceedings of the Cambridge Philosophical Society **35** (3) 416–418 (1939). DOI:10.1017/S0305004100021162
- H. Flaschka, *The Toda lattice. II. Existence of integrals*, Physical Review B **9** (4) 1924–1925 (1974). DOI:10.1103/PhysRevB.9.1924
- É. Forest, R. D. Ruth, *Fourth-order symplectic integration*, Physica D: Nonlinear Phenomena **43** (1) 105–117 (1990). DOI:10.1016/0167-2789(90)90019-L
- E. Hairer, C. Lubich, G. Wanner, *Geometric numerical integration: structure-preserving algorithms for ordinary differential equations*, 2nd ed., Springer (2006). DOI:10.1007/3-540-30666-8
- E. Hairer, S. P. Nørsett, G. Wanner, *Solving ordinary differential equations I: nonstiff problems*, 2nd ed., Springer (1993). DOI:10.1007/978-3-540-78862-1
- E. Hairer, G. Wanner, *Solving ordinary differential equations II: stiff and differential-algebraic problems*, 2nd ed., Springer (1996). DOI:10.1007/978-3-642-05221-7
- P. C. Hammer, J. W. Hollingsworth, *Trapezoidal methods of approximating solutions of differential equations*, Mathematical Tables and Other Aids to Computation **9** (51) 92–96 (1955). DOI:10.2307/2002064
- M. Hénon, *Integrals of the Toda lattice*, Physical Review B **9** (4) 1921–1923 (1974). DOI:10.1103/PhysRevB.9.1921
- A. Iserles, *A first course in the numerical analysis of differential equations*, 2nd ed., Cambridge University Press (2008). DOI:10.1017/CBO9780511995569
- W. Kutta, *Beitrag zur näherungsweise Integration totaler Differentialgleichungen*, Zeitschrift für Mathematik und Physik **46**, 435–453 (1901). [in German]
- L. D. Landau, E. M. Lifshitz, *Mechanics*, 3rd ed., Butterworth-Heinemann (1976).
- F. M. Lasagni, *Canonical Runge–Kutta methods*, Zeitschrift für angewandte Mathematik und Physik **39** (6) 952–953 (1988). DOI:10.1007/BF00945133
- P. D. Lax, *Integrals of nonlinear equations of evolution and solitary waves*, Communications on Pure and Applied Mathematics **21** (5) 467–490 (1968). DOI:10.1002/cpa.3160210503
- J. Mathews, R. L. Walker, *Mathematical methods of physics*, 2nd ed., Addison-Wesley (1970).
- R. H. Merson, *An operational method for the study of integration processes*, in *Proceedings of a conference on Data processing and automatic computing machines*, Weapons Research Establishment, Salisbury, Australia (1957), pp. 110–1–26.
- R. Penrose, *Applications of negative dimensional tensors*, in *Combinatorial Mathematics and its Applications*, ed. D. J. A. Welsh, Academic Press (1971), pp. 221–244.
- L. Poinso, *Théorie nouvelle de la rotation des corps*, Bachelier (1834). [in French]
- J. M. Sanz-Serna, *Runge–Kutta schemes for Hamiltonian systems*, BIT **28** (4) 877–883 (1988). DOI:10.1007/BF01954907
- Yu. B. Suris, *On the conservation of symplectic structure in numerical solution of Hamiltonian systems*, in *Numerical solution of ordinary differential equations*, ed. S. S. Filippov, Keldysh Institute of Applied Mathematics (1988), pp. 148–160. [in Russian]

- Yu. B. Suris, *The canonicity of mappings generated by Runge–Kutta type methods when integrating the systems $\dot{\mathbf{x}} = -\partial U/\partial \mathbf{x}$* , USSR Computational Mathematics and Mathematical Physics **29** (1) 138–144 (1989). DOI:10.1016/0041-5553(89)90058-X
- M. Suzuki, *Fractal decomposition of exponential operators with applications to many-body theories and Monte Carlo simulations*, Physics Letters A **146** (6) 319–323 (1990). DOI:10.1016/0375-9601(90)90962-N
- M. Toda, *Vibration of a chain with nonlinear interaction*, Journal of the Physical Society of Japan **22** (2) 431–436 (1967). DOI:10.1143/JPSJ.22.431
- H. Yoshida, *Construction of higher order symplectic integrators*, Physics Letters A **150** (5–7) 262–268 (1990). DOI:10.1016/0375-9601(90)90092-3

Appendix

Below is Wolfram Mathematica script that validates the three families of Runge–Kutta methods corresponding to the points $(c_2, c_3) = A, A',$ and A'' , and indexed by a parameter ψ . The output is zero matrix and zero vector to confirm the expressions, four zero vectors standing for $D(1)$, $D(c)$, $D(c^2)$, and $D(Ac)$, plus vector $\begin{bmatrix} 1 & \frac{1}{2} & \frac{1}{3} & \frac{1}{6} & \frac{1}{4} & \frac{1}{8} & \frac{1}{12} & \frac{1}{24} \end{bmatrix}$, to show that the order conditions are satisfied. The script exactly follows the derivation steps in Section 2.

```
A = {{ 0, 0, 0, 0, 0, 0, 0, 0},
      {c2, 0, 0, 0, 0, 0, 0, 0},
      {a31, a32, 0, 0, 0, 0, 0, 0},
      {a41, a42, a43, 0, 0, 0, 0, 0},
      {a51, a52, a53, a54, 0, 0, 0, 0},
      {a61, a32, 0, a64, a65, 0, 0, 0},
      {a71, 0, a73, a74, a75, a73, 0, 0},
      {a81, a82, a83, a84, a85, a86, a87, 0}}
b = {b1, b2, b3, b4, b5, b3, b2, b1}
c = {0, c2, c3, 1/2, 1/2, 1-c3, 1-c2, 1}
u = {1, 1, 1, 1, 1, 1, 1, 1}
SOLVE[e_, v_] := Set @@@ Simplify[Solve[e, v]][[1]]
Ap1 = Simplify[A.(2*c - u)]
SOLVE[Ap1[[2]] == Ap1[[7]], a71]; SOLVE[Ap1[[3]] == Ap1[[6]], a61]
Dp1 = Simplify[(b*(2*c - u)).A + b*Ap1]
SOLVE[Dp1[[1]] == 0, a81]; SOLVE[Dp1[[2]] == 0, a82]
SOLVE[Dp1[[7]] == 0, a87]; SOLVE[Ap1[[8]] == 0, a86]
SOLVE[(A.u)[[3]] == c[[3]], a31]
D1 = Simplify[b.A + b*(c - u)]
SOLVE[D1[[6]] == 0, Dp1[[6]] == 0], {a73, a83}]
SOLVE[(A.u)[[6]] == c[[6]], a64]
Ap2 = Simplify[A.(6*c^2 - 6*c + u)]; SOLVE[Ap2[[3]] + Ap2[[6]] == 0, a32]
SOLVE[(A.u)[[4]] == c[[4]], a41]; SOLVE[Ap2[[4]] == 0, a42]
Aq1 = Simplify[A.(A.c - (c^2)/2)]; SOLVE[Aq1[[4]] == 0, a43]
SOLVE[(A.u)[[5]] == c[[5]], a51]; SOLVE[Ap2[[5]] == 0, a54]
SOLVE[(A.u)[[7]] == c[[7]], a74]; SOLVE[Ap2[[2]] + Ap2[[7]] == 0, b3]
SOLVE[(A.u)[[8]] == c[[8]], a84]; SOLVE[Ap2[[8]] == 0, b1]
SOLVE[D1[[5]] == 0, a85]; SOLVE[b.u == 1, b4]; SOLVE[b.(c^2) == 1/3, b2]
SOLVE[Dp1[[5]] == 0, a75]; SOLVE[D1[[2]] == 0, a52]; SOLVE[D1[[3]] == 0, a53]
Dc2 = Simplify[(b*(c^2)).A + b*(A.(c^2) - u/3)]; SOLVE[Dc2[[5]] == 0, a65]
SOLVE[A[[5, 1]] == psi*c2, b5]
chi = 4*(1 - 3*c2) / ((1 - 6*c2)*(1/(2*c2) - 1 - psi))
z64 = 2*(1/2 - c3)*(1 - chi); z65 = 2*(1/2 - c3)*chi
z74 = 2*c2*(1 + chi); z75 = -2*c2*chi
Z = {{0, 0, 0, 0, 0, 0, 0, 0}, {c2, 0, 0, 0, 0, 0, 0, 0},
      {0, c3, 0, 0, 0, 0, 0, 0}, {1/2 - c2, c2 + c3 - 1, 1 - c3, 0, 0, 0, 0, 0},
      {psi*c2, (1 - psi)*c3, psi*(1/2 - 2*c2), psi*c2 + (1 - psi)*(1/2 - c3),
      0, 0, 0, 0}, {0, c3, 0, z64, z65, 0, 0, 0}, {c2, 0, 1/2 - 2*c2, z74, z75,
      1/2 - 2*c2, 0, 0}, {0, c3, 0, z64, z65, 0, c3, 0}}
y = {c2, c3, 1/2 - 2*c2, z64 + z74, z65 + z75, 1/2 - 2*c2, c3, c2}/2
Print["{A - Z, b - y, D1, Dp1, Dc2, DAC} = ",
      Simplify[{A - Z, b - y, D1, Dp1, Dc2, (b*(A.c)).A + b*(A.(A.c) - u/6)},
      Assumptions->{c2*(c2 - 1/2)*(c2 - 1) == 1/24, 6*c3*(1 - 2*c2)^2 == 1}]]
ORD = {u, c, c^2, A.c, c^3, c*(A.c), A.(c^2), A.(A.c)}
Print["ORD = ", Simplify[b.Transpose[ORD]]]
```

The expressions for A and b are confirmed in such a fashion because, *e.g.*, even assuming that $c_2(c_2 - \frac{1}{2})(c_2 - 1) = \frac{1}{24}$ and $6c_3(1 - 2c_2)^2 = 1$, due to details of implementation, the coefficient $a_{32} = (6c_3 - 1)/24c_2(1 - c_2)$ is unchanged by `Simplify` and `FullSimplify` commands, while $a_{32} - c_3$ is correctly simplified to 0.